Immunohistochemical detection of putative pathogenetic factors in adhesions of infants: a pilot study

Arvis Pauliņš, Anna Junga, Māra Pilmane

Institute for Anatomy and Anthropology, Rīga Stradiņš University, Riga, Latvia

ABSTRACT

Newborns' intestinal adhesions have been reported in 4.7% infants who underwent a laparotomy, but adhesions can also appear idiopathically. Etiology and pathogenesis of adhesions is still to be determined, but evidence shows relation to inflammation, formation of fibrin bands, hypoxia and tissue remodelation. Multiple candidate genes have been associated with adhesion development. The aim of this study was to evaluate the appearance of Sonic Hedgehog (SHH), Indian Hedgehog (IHH), Forkhead-box F1 (FOXF1), caudal type homeobox 1 (CDX1), HCLS1-associated protein X-1 (HAX-1), GATA Binding Protein 4 (GATA4) and Granzyme-B (GZMB) proteins in infant adhesions and to describe possible interfactorial correlations. Adhesion affected tissue samples were collected from 14 patients under one year of age that underwent abdominal surgery to treat partial or complete intestinal obstruction. The control group consisted of 6 individuals that had surgical repairment of inguinal hernia. Routine staining and immunohistochemistry were performed. Immunopositive fibroblasts, macrophages, endotheliocytes, smooth muscle myocytes of blood vessel wall and mesotheliocytes were investigated. The relative distribution of all factors was evaluated by the semiquantitative counting method. Statistical analysis was done using non-parametric tests and correlations were calculated based on Spearman's correlation analysis. A statistically significant decrease was observed for SHH, IHH, FOXF1, GATA4 and partially for GZMB in the adhesion group. There were also decreased HAX-1 and CDX1 immunopositive structures in the adhesion group, however, without any statistical significance. SHH, IHH, FOXF1, GATA4 and GZMB might have a role in adhesion development among infant patients which could suggest a dysregulation of cellular events. Abundance of correlations between the gene protein appearances in different structures indicate the affected blood vessels, fibroblasts and macrophages, however, mesothelium seems not to be the key driver in the morphopathogenesis of adhesion development.

Key words: gene proteins; immunohistochemistry; adhesions; infants.

Correspondence: Arvis Pauliņš, Institute for Anatomy and Anthropology, Rīga Stradiņš University, Dzirciema street 16, Riga, LV-1007, Latvia. E-mail: arvis.paulins@rsu.lv

Contributions: Arvis Pauliņš, formal analysis, software, visualization, writing - original draft, review and editing. Anna Junga, data curation, investigation, methodology, resources; Māra Pilmane, conceptualization, data curation, investigation, methodology, resources, funding acquisition, project administration, supervision, validation, writing - review and editing.

Conflicts of interest: the authors have no conflicts of interest to disclose.

Ethical approval: this research study was approved by Rīga Stradiņš University Ethical committee on 10.05.2007. During the study all regulations mentioned in the Helsinki Declaration were followed.

Availability of data and materials: the data used and analyzed in this research are presented in the results section of this study.

Introduction

Intestinal adhesion formation is a natural and inevitable part of post-operative period. Different studies show that it is present in approximately 90% of cases following open intra-abdominal surgery.[1,2] It can be associated with infections and inflammation as well, for example, peritonitis, and it can also be congenital - without any previous surgical intervention associations.[3] The nature of surgical interventions in pediatric patients, especially infants, possess a significantly higher risk of adhesion-related complications. Intestinal adhesions are a major cause of, for example, adhesive small bowel obstruction (ASBO), which has been reported in 4.7% infants that underwent a laparotomy.[4,5]

Intra-abdominal adhesions are conjunctions of connective tissue that can develop between any organ surfaces in the peritoneal cavity.[6] Their morpho-pathogenesis is still not fully understood yet, but evidence shows that it can be associated with inflammatory processes and formation of fibrin matrix bands, hypoxia of tissue and reduction in fibrinolytic cascade activity, it all resulting to tissue extracellular matrix remodelation and accumulation with altered expression of various modulating factors that determine and regulate tissue growth.[7] All of these processes depend on the genes and their products' influence in both pre- and post-natal periods. Some of the most important factors regulating tissue development during embryogenesis are the Hedgehog genes - Sonic Hedgehog (*SHH*) and Indian Hedgehog (*IHH*). They are involved in the organogenesis of many different tissues, such as central nervous system, eye, axial skeleton, limbs, tooth, hair follicles, lung, liver, kidney and gut. *SHH* also participates in regulating left-right asymmetry of visceral organs.[8,9]

A morphogen is another term used when describing a Hedgehog gene. It means that *SHH* and *IHH* effects are dependent on their expressed protein concentration around their target cells and their distance from the structures that secrete the Hedgehog protein.[8,10,11] Different concentration thresholds lead the target cells into different fates (proliferation, growth arrest, differentiation, programmed cell death or migration) by either activating or suppressing the intracellular Hedgehog signaling pathway, which affects the Hedgehog target genes' expression at distinct time and places in the embryo.[12,13] In early developmental stages it is expressed in the early gut endoderm, throughout the notochord and other structures, which corresponds to expression in fetal intestine, liver, lung, and kidney in the later stages of embryogenesis.[1]. A very low level of Hedgehog postnatal expression has been detected in adult stomach, distal colon and possibly other regions, where it is thought to have a role in maintenance of tissue homeostasis or so called morphostasis.[11] SHH is one of the ligands in the intracellular Hedgehog signaling pathway, which is an important regulatory pathway in early embryogenesis in most animals, including *Homo sapiens*. Alterations in Hedgehog expression may contribute to pathological adhesion development.

Forkhead-box F1 (*FOXF1*), also known as Hepatocyte Nuclear Factor 8 (HFH8) or Forkhead Related Activator 1 (FREAC-1), is a member of the human FOX gene family located on chromosome 16q24.1. The expression of *FOXF1* begins during gastrulation in extraembryonic mesoderm, allantois, and lateral mesoderm and continues in splanchnic (visceral) mesoderm, which is critical for the mesenchymal/epithelial induction of gut-derived organs, such as the liver, gallbladder, lung, stomach, and intestine. *FOXF1* in developing mouse embryo has been detected in stomach and intestine dependently on N-SHH protein induced glioma-associated oncogene 2 (Gli2) and Gli3 expression, although a total absence of Glis does not completely extinguish *FOXF1* expression in the developing gut.[15] It is thought that *FOXF1* deficiency in the intestine could be the reason for defects in cell migration during villus development, which in turn can affect the epithelial organization and distribution along the crypt-villus axis.[15,16] *FOXF1* also has an essential role in normal midgut rotation by leading the formation of the dorsal mesentery in generating the left-right asymmetry that allows rotation to take place.[17]

Caudal type homeobox 1 *(CDX1)* (5q32) is a protein-coding gene belonging to the so-called caudal genes. *CDX1* is expressed in the developing endoderm, where its expression also persists postnatally - mainly in the distal colon and along the crypt-villus axis in the region of intestinal crypts.[18,19] *CDX1* is an intestine-specific transcription factor that directs the maturation and differentiation of enterocytes and the maintenance of intestinal phenotype in general. CDX transcription factors act as crucial effectors for activating central Hox genes.[20]

HCLS1-associated protein X-1 *(HAX-1)* seems to play an inhibitory role in apoptosis, the organization of the cytoskeleton and molecule shuttle. In jejunum it is mainly expressed in epithelial cells of crypts and villi.[21,22] Specific functions of *HAX-1* during embryogenesis are still not fully understood.

GATA Binding Protein 4 *(GATA4)* (8p23.1) encodes a member of the GATA family of zinc-finger transcription factors. *GATA4* is expressed in the midgut endoderm during embryogenesis and in both crypt and villus enterocytes of duodenum and jejunum but not ileum throughout adulthood.[23-25] In jejunum *GATA4* plays an essential role in regulating enterocyte jejunal-specific gene expression, cytodifferentiation and maintenance of the jejunal-type enterocyte identity, while suppressing ileal-type enterocyte identity. *GATA4* expression is required in jejunum for normal fat and cholesterol absorption. Moreover, it is suggested that *GATA4* contributes to intestinal epithelial cell fate decisions by modulation Notch signaling through the regulation of delta like canonical Notch ligand 1 (Dll1).[26]

Granzyme-B (*GZMB*, 14q12) is a protein coding gene from granzyme gene family. It encodes a pro-apoptotic protein that is a part of the peptidase S1 family of serine proteases - a granzyme subfamily of proteins. GZMB is currently recognized for its intracellular roles in immune cell-mediated apoptosis as well as extracellular roles in inflammation, chronic injuries, tissue remodeling, as well as processing of cytokines, matrix proteins, and autoantigens.[27] The active form of GZMB induces target cell apoptosis via two kinds of apoptotic cell death, the intracellular perforin-dependent apoptosis and the extracellular perforin-independent apoptosis, called anoikis. Anoikis is characterized with apoptosis induced by disruption of the interactions between normal epithelial cells and extracellular matrix. It does not occur in normal fibroblasts.[28] GZMB also processes cytokines and degrades extracellular matrix proteins, such as fibronectin, vitronectin, laminin, SMC matrix, VE-cadherin, fibrillin-1, proteoglycan, biglycan and decorin, and these roles are implicated in chronic inflammation and wound healing. Likewise, GZMB promotes impaired epithelial function of the gut and other organs. GZMB is one of the drivers of the activation of pro-inflammatory, pro-fibrotic and aging mediators belonging to the IL-1 cytokine family.[29]

The formation of adhesions may involve a multifaceted interplay of various morpho-pathogenetic factors. A better understanding of it at the cellular and molecular levels would help to develop more effective and targeted treatment and prevention strategies for adhesions. Although, a lot of factors have been studied before, the data is scarce, therefore, in order to extend the knowledge on basis of above mentioned, the aim of this study was to determine the relative quantity of specific gene products (SHH, IHH, FOXF1, CDX1, HAX-1, GATA4, GZMB) and their distribution in infant

patients' intestinal adhesion tissue and to find possible interfactorial correlations that might be involved in the formation and development of adhesions.

Materials and Methods

Characteristics of subjects

This research study was done in the Institute of Anatomy and Anthropology (IAA) of Rīga Stradiņš University (RSU) Department of Morphology, Latvia. It was approved by RSU Ethical committee on 10.05.2007. During the study all regulations mentioned in the Helsinki Declaration were followed.

Fourteen intestinal adhesion tissue samples in the size of approximately 1-2 mm were collected at the Department of Children Surgery from infant patients, from which 9 were females and 5 were males, ageing from 1 to 134 days. The most common pathologies among the patients were intestinal rotation disorders (six cases) and presence of Ladd's bands (four cases), as well as gastroschisis (four cases). The most common place of adhesions was the jejunum or the proximal ileum (seven cases). Detailed information about the patients can be seen in Table 1. The samples were included from patients that underwent abdominal surgery to treat partial or complete intestinal obstruction.

Parents or legal guardians of study groups' patients gave authorization and permission for the tissue sampling and research conduction.

Characteristics of control group

Six samples in the size of approximately 3-4 mm for control group were collected at Department of Children Surgery. The control group consists of four males and two females, ageing from 46 to 92 days. Information about the control group is shown in Table 2. The control group's inclusion criterion was surgical repairment of inguinal hernia. Parents or legal guardians of control

Table 1. Description of patients in the adhesion group.

No.	Sex	Age (days)	Adhesion place	Diagnosis
1	F	1	LB	Meconium ileus, Ladd's ligament, rotation disorders of the intestinal tract
2	F	1	LB	Left-sided diaphragmatic hernia, Ladd's ligament
3	M	2	JI	Intrauterine ileus with volvulus at the distal end of the ileum, necrosis of the caecum. Ileostomy
4	M	2	D	Atresia of the ileum
5	M	3	LB	Malrotation of the intestinal tract, volvulus of the small intestine (360°) with perfusion disorders in the distal ileum (16 cm), Ladd's ligament. Ileostomy (T)
6	M	4	D	Intestinal rotation disorders, partial patency of the gastrointestinal tract, congenital peritoneal adhesions in the duodenal region
7	F	9	D	Gastroschisis
8	M	14	JI	Gastroschisis. Condition after plastic surgery of the anterior wall of abdomen. Adhesion ileus
9	F	51	LB	Intestinal rotation disorders, congenital peritoneal adhesions, Ladd's ligament
10	F	56	JI	Gastroschisis. Condition after plastic surgery of the anterior wall of abdomen, condition after ileostomy (T) placement
11	F	56	JI	Gastroschisis. Condition after plastic surgery of the anterior wall of abdomen, condition after ileostomy (T) placement
12	F	71	JI	Volvulus of the small intestine (360°), condition after partial obstruction of the gastrointestina tract, rupture of Ladd's ligament
13	F	94	JI	Partial impermeability of the gastrointestinal tract, condition after diaphragmatic hernia surgery
14	F	134	JI	Partial impermeability of the gastrointestinal tract. Condition after mesenteric thrombosis, condition after partial resection of jejunum, total resection of ileocecal angle and ascending colon, condition after application and closure of jejuno-transversostomy

LB, Ladd's bands; D, duodenum; JI, jejunum and the proximal part of ileum.

Table 2. Description of patients in the control group.

No.	Gender	Age (days)	Clinical diagnosis
1	F	46	Left side inguinal hernia
2	M	56	Right side inguinal hernia
3	F	60	Right side inguinal hernia
4	M	73	Left side inguinal hernia
5	M	76	Right side inguinal hernia
6	M	92	Right side inguinal hernia

groups' patients gave authorization and permission for the tissue sampling and research conduction.

Immunohistochemical (IHC) analysis

For tissue sample fixation a formaldehyde 2% solution was used together with 0.2% picric acid and 0.1M phosphate buffer at pH level 7.2. Then a washing process for 12 h was carried out using phosphate buffer, saline solution, and a 10% saccharose solution. Afterwards, the tissue samples were embedded in paraffin and sliced into thin sections measuring 5-7 µm. Finally, deparaffinization and sample staining was performed. Routine staining with haematoxylin and eosin was done in order to evaluate the general morphology of the samples. To detect and evaluate gene product presence and relative distribution tissue IHC staining was done by biotin-streptavidin standard method,[30] using these primary antibodies: anti-SHH antibodies (code ab53281, rabbit, working dilution 1:500, Abcam, Cambridge, UK); anti-IHH antibodies (code sc-271101, mouse, working dilution 1:100, Santa Cruz Biotechnology, Inc., Dallas, TX, USA); anti-FOXF1 antibodies (code orb522377, rabbit, working dilution 1:100, Biorbyt Ltd., Cambridge, UK); anti-CDX1 antibodies (code orb518774, rabbit, working dilution 1:100, Biorbyt Ltd.); anti-HAX-1 antibodies (code sc-166845, mouse, working dilution 1:100, Santa Cruz Biotechnology, Inc.); anti-GATA-4 antibodies (code sc-25310, mouse, working dilution 1:100, Santa Cruz Biotechnology, Inc.); anti-GZMB antibodies (code sc-8022, mouse, working dilution 1:100, Santa Cruz Biotechnology, Inc.). First, the antibodies were diluted using an antibody diluent (code-938B-05, Cell MarqueTM, Rocklin, CA, USA). After that deparaffinization of previously cut tissue samples, rehydration of samples in alcohol and water, rinsing with tris buffer solution (code-2017X12508, Diapath S.p.A., Martinengo, Italy) twice for 5 min each, heating the samples in a microwave with boiling EDTA buffer (code-2017X02239, Diapath S.p.A.) for 20 min and then cooling, washing with tris buffer 2 × 5 min, blocking with 3% peroxide for 10 min, and washing with tris buffer.

Finally, incubation of samples with above mentioned antibodies for 1 h, washing of samples with tris buffer three times, exposing the samples to the HiDef DetectionTM reaction amplifier (code 954D-31, Cell MarqueTM) for 10 min at room temperature, and washing with tris buffer three times for 5 min each. Hematoxylin was used for nuclear counterstaining. Positive controls were performed in accordance with the manufacturer's instructions, using the recommended tissues to verify antibody

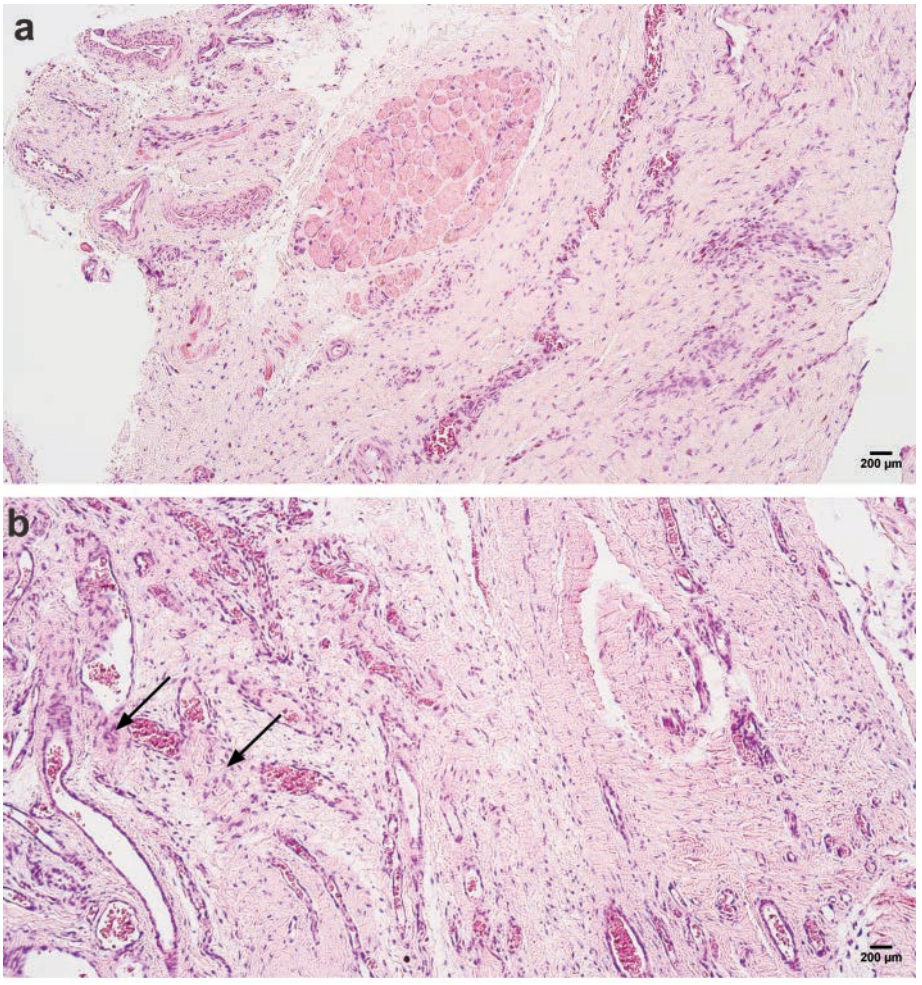

Figure 1. a) Control sample with normal morphology of intestinal wall tissue, hematoxylin and eosin, x100. **b**) Adhesion sample with chaotic architecture of connective tissue fibers, increased cellularity and infiltration of inflammatory cells (arrows), hematoxylin and eosin, X100.

specificity. Negative controls were prepared by omitting the primary antibody from the immunohistochemical protocol.

Sample analyzing by two independent raters was done with a light microscope (Leica DC 300F, Leica Biosystems, Richmond, VA, USA; 10x, 20x), the semi-quantitative scoring method[31] with certain non-parametric identifiers listed on Table 3. was applied for assessing the relative appearance and distribution of the immunopositive morphopathogenic factors in these tissue structures - mesothelium, fibroblasts, macrophages, endothelium and wall of blood vessels. A semi-quantitative scoring method is an evaluation approach that converts qualitative observations into ordinal numerical scores, it is widely used when precise quantitative measurement is impractical, but consistent, reproducible, and biologically meaningful comparison between groups is required. Because findings obtained by the raters showed minimal variation and near-complete agreement, additional inter-rater and intra-rater

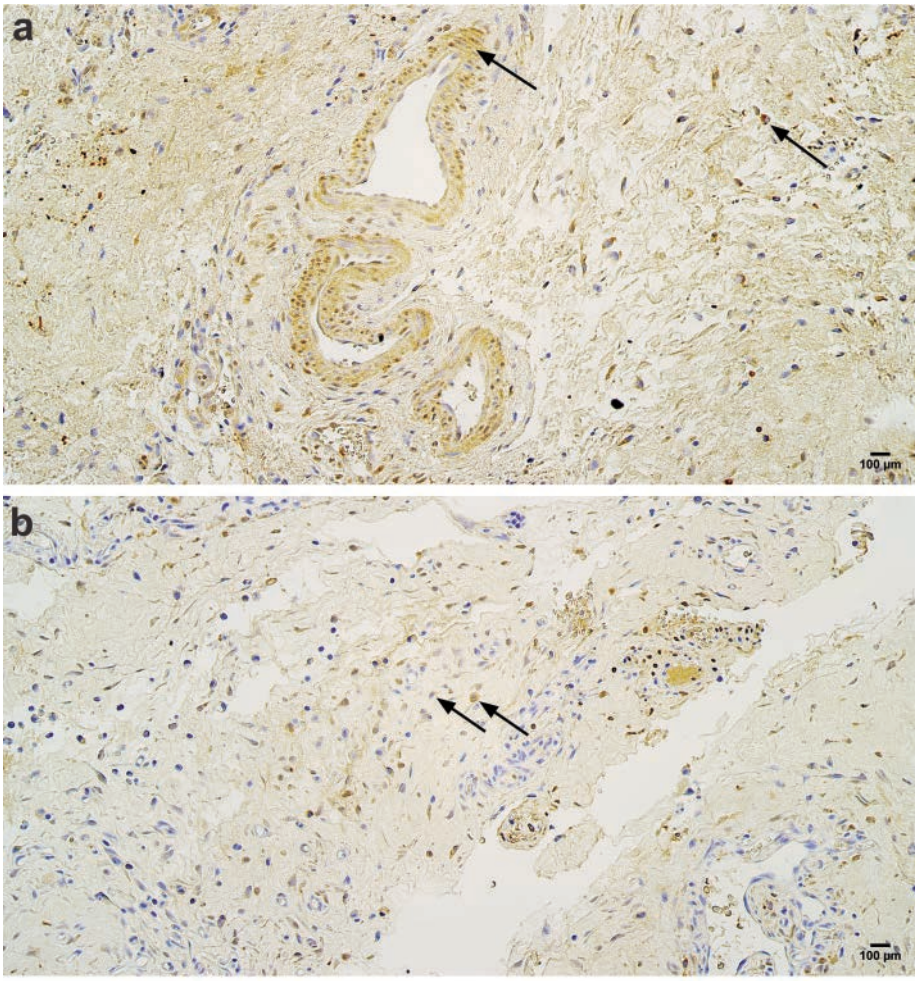

Figure 2. Immunopositive structures of SHH. **a**) Control sample with moderate number of SHH-immunopositive smooth muscle cells, fibroblasts and macrophages (arrows), SHH IHC, x200. **b**) Adhesion sample with few to moderate number of SHH-immunopositive fibroblasts and macrophages (arrows), but absence of SHH immunoreactivity in blood vessels, SHH IHC, x200.

Table 3. Semi-quantitative scoring identifiers used for relative frequency determination of immunopositive factors.

Legend	Description
0	No immunopositive factors in the visual field
0/+	Rare occurrence of immunopositive factors in the visual field
+	Few immunopositive factors in the visual field
+/++	Few to moderate number of immunopositive factors in the visual field
++	Moderate number of immunopositive factors in the visual field
++/+++	Moderate to abundant immunopositive factors in the visual field
+++	Abundance of immunopositive factors in the visual field

reliability analyses were considered unnecessary. Semi-quantitative scores were treated as ordered ordinal data, and median values across samples were calculated for each marker and reported using the corresponding identifier. For visual illustration photos of the sample slides were taken with a digital camera Leica DC 300F (Leica Microsystems Digital Imaging, Cambridge, UK) and processed with Image Pro Plus program (Media Cybernetics, Inc., Rockville, MD, USA).

Statistical analysis

All the data were statistically analyzed with program IBM SPSS version 26.0 (IBM Company, Chicago, IL, USA). Correlation analysis and non-parametric statistic tests were used. Spearman's rank correlation analysis was done, where $0.0 < R < 0.3$ indicated a negligible correlation, $0.3 < R < 0.5$ indicated a low positive correlation, $0.5 < R < 0.7$ indicated a moderate positive correlation, $0.7 < R < 0.9$ indicated a high positive correlation and $0.9 < R < 1$ indicated a very high positive correlation.[32] Statistical significance was determined with a Mann-Whitney U test between the controls and patient group. The p values less than 0.05 were considered statistically significant for all statistical tests.

Results

Routine staining

Control sample did not show any distinct changes from the standard loose connective tissue structure generally (Figure 1a). In all adhesion samples fibrous tissue with pronounced connective tissue fiber agglomerates was observed, as well as infiltration of inflammatory cells (lymphocytes, macrophages and gigantic cells) (Figure 1b). In samples where mesothelium could be identified (five cases), a rounded form of some mesothelial cells was noted.

IHC staining

SHH

In the control group the median quantity of SHH-immunopositive structures was few (+) mesotheliocytes, moderate number (++) of fibroblasts, endothelium and smooth muscle cells in the blood vessel wall, and moderate to abundant number (++/+++) of macrophages (Figure 2a). In adhesion group the median number of SHH-immunopositive structures was rare occurring (0/+) in

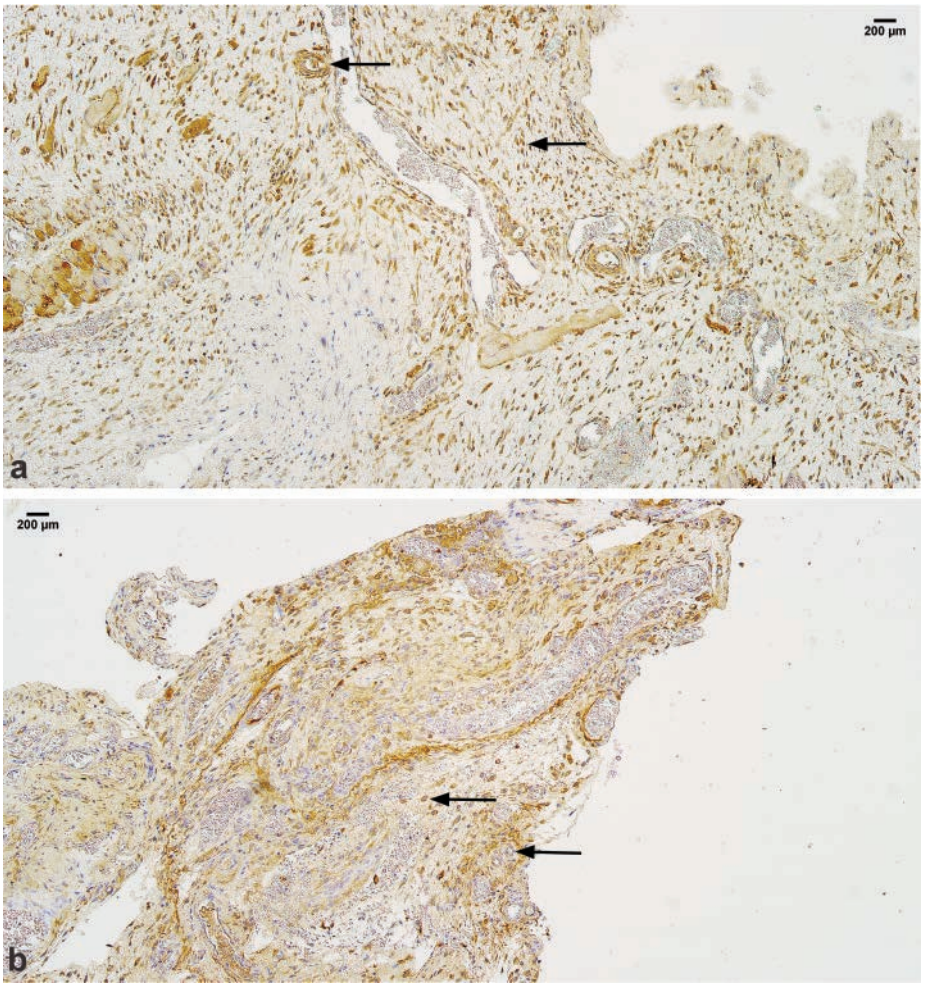

Figure 3. Immunopositive structures of IHH. **a**) Sample of control group with moderate to abundant IHH-immunopositive fibroblasts, macrophages and myocytes in blood vessels (arrows), IHC IHH, x100. **b**) Adhesion sample with few to moderate IHH-immunopositive fibroblasts, macrophages, endotheliocytes (arrows), IHC IHH, x100.

mesothelium, endothelium and in blood vessel walls, there were few (+) fibroblasts, and few to moderate number (+/++) of macrophages (Figure 2b). Statistical tests revealed that significantly less SHH-positive mesotheliocytes (U = 2.5, p=0.017), fibroblasts (U = 15.5, p=0.026) and structures in blood vessel walls (U = 5.0, p<0.001) were found in adhesion group when compared to controls (Table 4).

IHH

In the control group the median quantity of IHH-immunopositive structures was detected to be few to moderate number (+/++) of mesotheliocytes, while moderate to abundant number (++/+++) of fibroblasts, macrophages and smooth myocytes in blood vessel walls were seen, and abundant number of cells (+++) in endothelium (Figure 3a). In adhesion group the median number of IHH-immunopositive

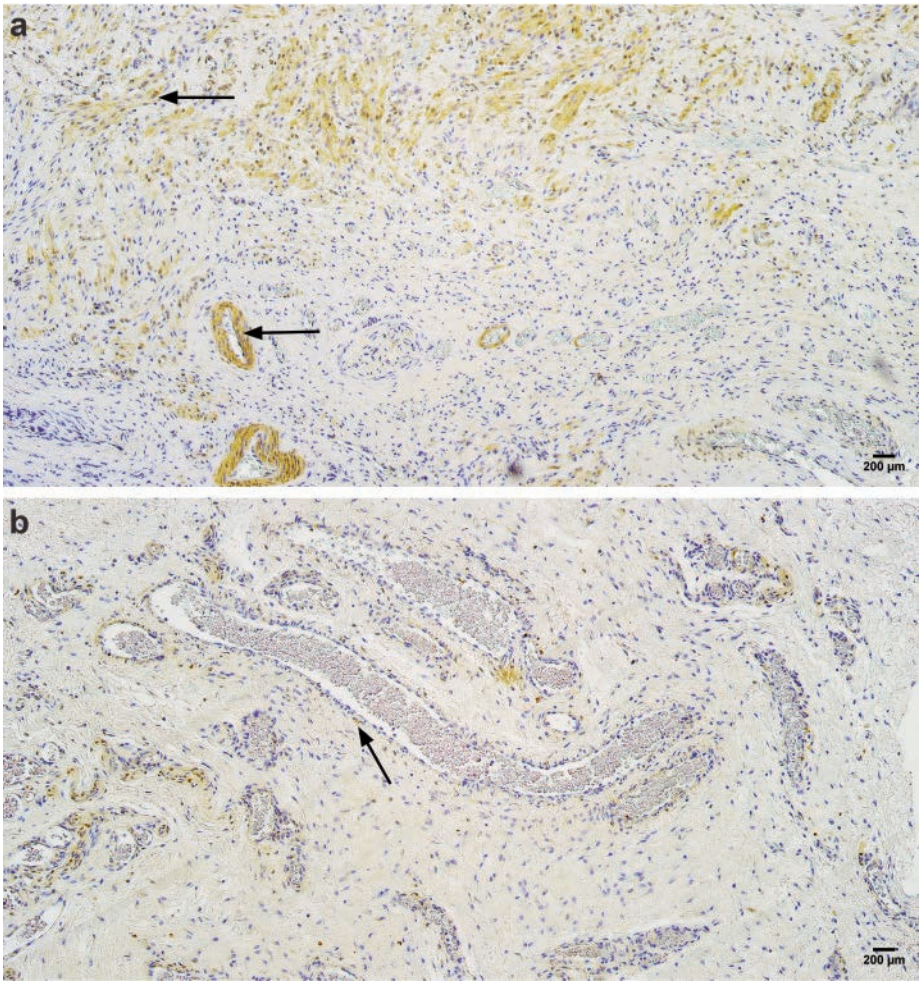

Figure 4. Immunopositive structures of FOXF1. **a)** Control sample with moderate number of FOXF1-immunopositive fibroblasts and myocytes in blood vessels (arrows), IHC FOXF1, x100. **b**) Adhesion sample with low intensity of rare occurring FOXF1-immunoreactive structures (arrow), IHC FOXF1, x100.

Table 4. Semiquantitative scoring of immunoreactivities of FOXF1, SHH, IHH, and GATA-4 in adhesion group and control group.

	Factors																			
	FOXF1					SHH					IHH					GATA-4				
Structure	Mt	F	Mp	E	BW	Mt	F	Mp	E	BW	Mt	F	Mp	E	BW	Mt	F	Mp	E	BW
Patients	0/+	+	0/+	0/+	0/+	0/+	+	+/++	0/+	0/+	0/+	0/+	0/+	0/+	0	0	0/+	0/+	0/+	0/+
Control	0/+	++	+/++	+/++	++	+	++	++/+++	++	++	+/++	++/+++	++/+++	+++	++/+++	0/+	++	++	++	++
U test	6.0	11.0	4.0	0.0	1.0	2.5	15.5	19.0	5.0	5.0	0.0	0.0	0.0	0.0	0.0	0.0	3.0	3.0	0.0	0.0
p value	0.548	0.009	<0.001	<0.001	<0.001	0.017	0.026	0.062	<0.001	<0.001	0.016	<0.001	<0.001	<0.001	<0.001	0.095	<0.001	<0.001	<0.001	<0.001

Mt, mesothelium; F, fibroblasts; Mp, macrophages; E, endothelium; BW, blood vessel wall; U test, Mann-Whitney U test value.

structures was of rare occurring (0/+) in all the studied histological structures, except in blood vessel walls, where a lack of (0) immunoreactivity was observed (Figure 3b). In the adhesion specimens immunopositive structures were found in significantly lower number ($U = 0.0$, $p<0.001$) for IHH than in control tissues (Table 4).

FOXF1

In the control group the median quantity of FOXF1-immunopositive structures was rare occurring (0/+) in mesothelium, few to moderate number (+/++) of macrophages and endothelium, a moderate number (++) of fibroblasts and myocytes in blood

Table 5. Semiquantitative scoring of immunoreactivities of GZMB, CDX1 and HAX-1 in adhesion group and control group.

Factors	Granzyme-B					CDX1					HAX-1				
Structure	**Mt**	**F**	**Mp**	**E**	**BW**	**Mt**	**F**	**Mp**	**E**	**BW**	**Mt**	**F**	**Mp**	**E**	**BW**
Patients	0/+	+/++	0/+	0/+	0/+	0/+	++	+/++	+	+	0	0/+	0/+	0	0
Control	+	++	+/++	+/++	+/++	0/+	+/++	+/++	+/++	+/++	0	0/+	0/+	0/+	0/+
U test	2.0	20.0	6.0	2.0	2.0	3.5	36.0	33.5	20.5	20.5	0	28.0	42.0	17.0	14.0
p value	0.381	0.076	0.002	<0.001	<0.001	0.429	0.659	0.494	0.076	0.076	0	0.274	1.000	0.041	0.020

Table 6. Statistically significant correlations between factors in patients' adhesion tissue samples based on Spearman's correlation analyses.

Factor 1	Factor 2	Spearman's rho	*p*
High positive correlations			
FOXF1 in endothelium	GATA4 in endothelium	0.765	<0.001
FOXF1 in blood vessels	GZMB in blood vessels	0.754	0.002
FOXF1 in blood vessels	CDX1 in blood vessels	0.771	<0.001
SHH in fibroblasts	SHH in macrophages	0.704	0.005
SHH in endothelium	SHH in blood vessels	0.773	<0.001
IHH in fibroblasts	IHH in macrophages	0.849	<0.001
GATA4 in fibroblasts	GATA4 in macrophages	0.803	<0.001
GATA4 in macrophages	HAX1 in macrophages	0.727	0.003
GATA4 in endothelium	CDX1 in endothelium	0.708	0.005
GATA4 in endothelium	GATA4 in blood vessels	0.891	<0.001
GZMB in fibroblasts	GZMB in macrophages	0.725	0.003
GZMB in endothelium	CDX1 in endothelium	0.727	0.003
CDX1 in fibroblasts	CDX1 in macrophages	0.831	<0.001
Moderate positive correlations			
FOXF1 in fibroblasts	FOXF1 in macrophages	0.537	0.048
FOXF1 in endothelium	SHH in macrophages	0.669	0.009
FOXF1 in endothelium	IHH in endothelium	0.686	0.007
FOXF1 in endothelium	GZMB in endothelium	0.563	0.036
FOXF1 in endothelium	CDX1 in endothelium	0.622	0.018
FOXF1 in endothelium	HAX1 in fibroblasts	0.536	0.048
SHH in macrophages	GATA4 in endothelium	0.590	0.026
IHH in fibroblasts	GATA4 in fibroblasts	0.668	0.009
IHH in macrophages	GATA4 in fibroblasts	0.536	0.048
IHH in macrophages	GZMB in fibroblasts	0.540	0.046
IHH in endothelium	GZMB in endothelium	0.603	0.023
IHH in endothelium	HAX1 in fibroblasts	0.549	0.042
GATA4 in fibroblasts	HAX1 in macrophages	0.626	0.017
GATA4 in macrophages	GZMB in fibroblasts	0.597	0.024
GATA4 in endothelium	GZMB in endothelium	0.562	0.036
GATA4 in blood vessels	SHH in fibroblasts	0.591	0.026
GATA4 in blood vessels	CDX1 in blood vessels	0.622	0.017
HAX1 in fibroblasts	HAX1 in macrophages	0.627	0.017

vessel walls was seen (Figure 4a). In the adhesion samples the median number of FOXF1-immunopositive structures was of rare occurring (0/+) in mesothelium, endothelium and blood vessel walls, also just rare macrophages and few (+) fibroblasts were seen (Figure 4b). Compared to control group, a statistically significant decrease in the number of immunopositive fibroblasts (U = 11.0, p=0.009), macrophages (U = 4.0, p<0.001) and blood vessels (U = 1.0, p<0.001) was observed in adhesion group (Table 4).

CDX1

In the control samples the median quantity of CDX1-immunopositive structures was rare occurring (0/+) in mesothelium, moderate number (++) of fibroblasts, macrophages, endothelium and myocytes in blood vessel walls was detected (Figure 5a). In the adhesion samples the median number of CDX1-immunopositive structures was rare occurring (0/+) in mesothelium, few (+) in blood vessel wall, few to moderate number (+/++) of macrophages, and moderate number (++) fibroblasts was detected (Figure 5b). The number of the observed positive mesotheliocytes (U = 3.5, p=0.429), fibroblasts (U = 36.0, p=0.659), macrophages (U = 33.5, p=0.494) and blood vessels (U = 20.5, p=0.076) was not significantly different in comparison to the control group tissues (Table 5).

HAX-1

In the control samples the median number of HAX-1 immunopositive structures was rare occurring (0/+), except for mesothelium where absence (0) of any immunoreactive structures was detected (Figure 6a). In the adhesion samples only rare number (0/+) of HAX-1 immunopositive fibroblasts and macrophages were found. No other HAX-1 immunoreactive (0) structures were observed (Figure 6b). In adhesion group a statistically significant decrease in the number of immunopositive blood vessels (U = 14.0, p=0.020) was seen when comparing to control group (Table 5).

GATA4

In the control samples the median number of GATA4 immunoreactive structures was moderate (++), except mesothelium where only rare occurrence (0/+) of immunopositive cells was detected (Figure 7a). In the adhesion samples the median number of GATA4 immunopositive structures was rare occurring (0/+), except for mesothelium, which lacks (0) GATA4 immunoreactivity completely (Figure 7b). A statistically significant lower number of fibroblasts (U = 3.0, p<0.001), macrophages (U = 3.0, p<0.001) and blood vessels (U = 0.0, p<0.001) was observed in adhesion group when compared to controls (Table 4).

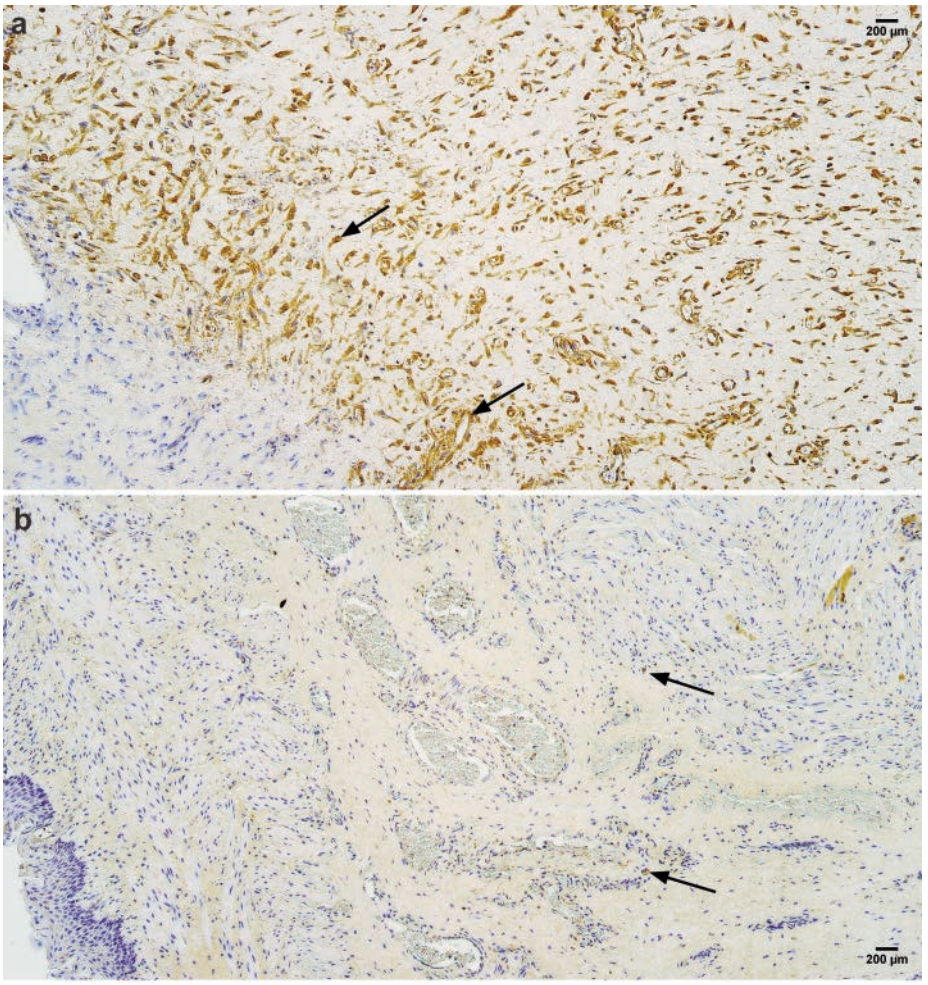

Figure 5. Immunopositive structures of CDX1. **a**) Control sample with moderate number of CDX1-positive structures (arrows), IHC CDX1, x100. **b**) Adhesion sample with few CDX1-immunopositive fibroblasts and macrophages (arrows), IHC CDX1, x100.

GZMB

In the control samples the median quantity of GZMB-immunopositive structures was few (+) in mesothelium, few to moderate number (+/++) of macrophages and myocytes in blood vessels, and moderate number (++) of fibroblasts was detected (Figure 8a). In the adhesion samples the median number of GZMB-immunopositive structures was rare (0/+), except few to moderate number (+/++) of immunoreactive fibroblasts were found (Figure 8b). Between the control and the adhesion group a statistically significant decrease in the number of immunopositive macrophages (U = 6.0, p=0.002) and blood vessels (U = 2.0, p<0.001) was observed (Table 5).

Correlations

Spearman correlation analysis showed statistically significant correlations for these factors in the adhesion group: a strong positive correlation was seen between the number of FOXF1 immunopositive endotheliocytes and GATA4 immunopositive endotheliocytes (Spearman's rho = 0.765, p<0.001); between FOXF1 immunopositive blood vessels and GZMB immunopositive blood vessels (Spearman's rho = 0.754, p=0.002); between FOXF1 immunopositive blood vessels and CDX1 immunopositive blood vessels (Spearman's rho = 0.771, p<0.001); between the number of SHH immunopositive fibroblasts and SHH immunopositive macrophages (Spearman's rho = 0.704, p=0.005); between the number of SHH immunopositive endotheliocytes and SHH immunopositive cells in blood vessels (Spearman's rho = 0.773, p<0.001); between IHH immunopositive fibroblasts and macrophages (Spearman's rho = 0.849, p<0.001); between the number of GATA4 immunopositive fibroblasts and macrophages (Spearman's rho = 0.803, p<0.001); between GATA4 immunopositive fibroblasts and HAX-1 immunopositive macrophages (Spearman's rho = 0.727, p=0.003); between GATA4 immunopositive endotheliocytes and CDX1 immunopositive endotheliocytes (Spearman's rho = 0.708, p=0.005); between the number of GATA4 immunopositive endotheliocytes and cells in blood vessels (Spearman's rho =0.891, p<0.001); between GZMB immunopositive fibroblasts and macrophages (Spearman's rho =0.725, p=0.003); between the number of GZMB immunopositive endotheliocytes and CDX1-positive endotheliocytes (Spearman's rho =0.727, p=0.003); between CDX1 immunopositive fibroblasts and macrophages (Spearman's rho = 0.831, p<0.001). No important correlations were seen for mesothelium. A summary of statistically significant Spearman's correlations is shown in Table 6.

Statistical calculations also showed significant moderate positive correlations in the adhesion group between the following factors: FOXF1-positive fibroblasts and macrophages (Spearman's rho = 0.537, p=0.048); between FOXF1-positive endotheliocytes and SHH-positive macrophages (Spearman's rho =0.669, p=0.009); between FOXF1-positive endotheliocytes and IHH-positive endotheliocytes (Spearman's rho = 0.686, p=0.007); between FOXF1-positive endotheliocytes and GZMB-positive endotheliocytes (Spearman's rho =0.563, p=0.036); between FOXF1-positive endotheliocytes and CDX1-positive endotheliocytes (Spearman's rho = 0.622, p=0.018); between FOXF1-positive endotheliocytes and HAX-1-positive fibroblasts (Spearman's rho = 0.536, p=0.048); between SHH-positive macrophages and GATA4-positive endotheliocytes (Spearman's rho =0.590, p=0.026); between

Table 7. Correlations between gene proteins in patient adhesion tissue samples based on Spearman's correlation analysis.

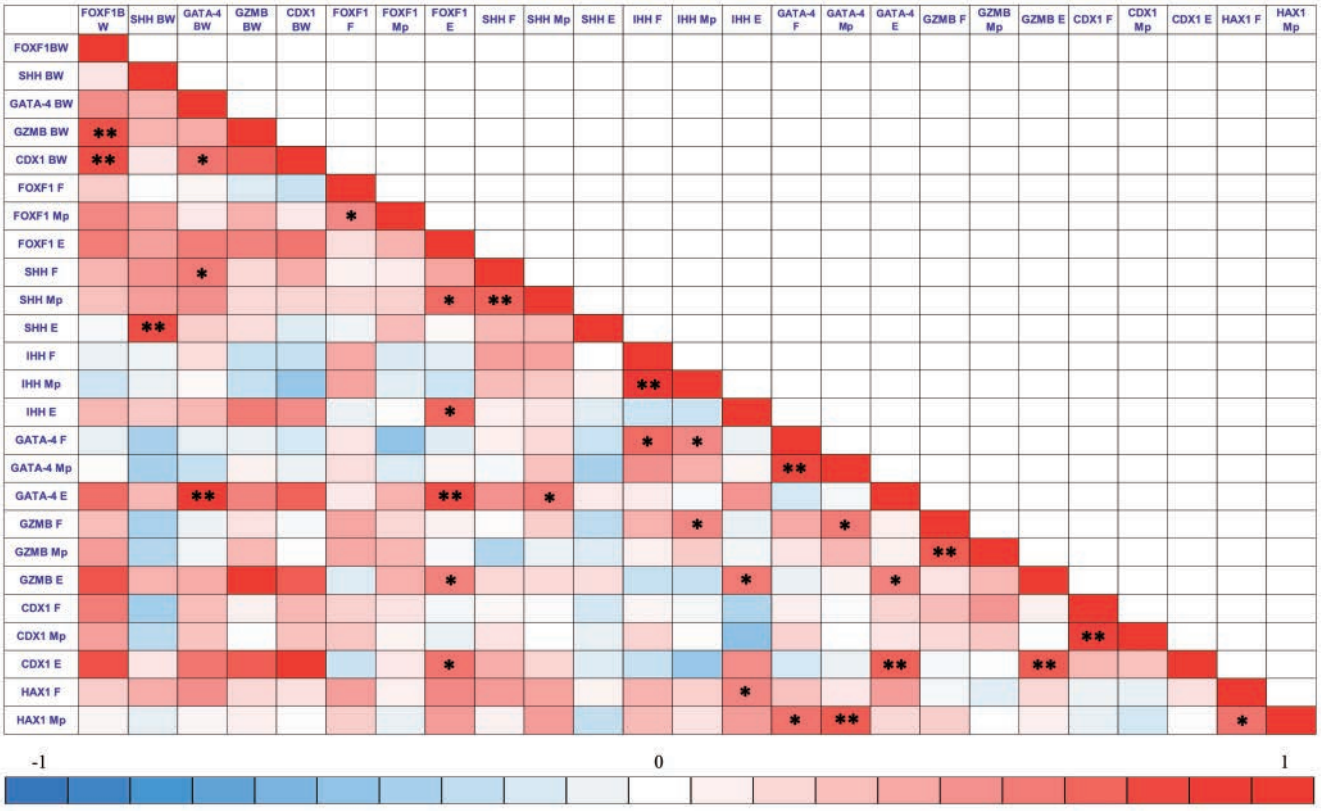

IHH-positive and GATA4-positive fibroblasts (Spearman's rho = 0.668, p=0.009); between IHH-positive macrophages and GATA4-positive fibroblasts (Spearman's rho = 0.536, p=0.048); between IHH-positive macrophages and GZMB-positive fibroblasts (Spearman's rho = 0.540, p=0.046); between IHH- and GZMB-positive endotheliocytes (Spearman's rho = 0.603, p=0.023); between IHH-positive endotheliocytes and HAX-1-positive fibroblasts (Spearman's rho = 0.549, p=0.042); between GATA4-positive fibroblasts and HAX-1-positive macrophages (Spearman's rho = 0.626, p=0.017); between GATA4-positive macrophages and GZMB-positive fibroblasts (Spearman's rho = 0.597, p=0.024); between GATA4- and GZMB positive endotheliocytes (Spearman's rho = 0.562, p=0.036); between the number of GATA4 immunopositive cells in blood vessels and SHH-positive fibroblasts (Spearman's rho = 0.5941, p=0.026); between the number of GATA4 and CDX1 immunopositive cells in blood vessels (Spearman's rho = 0.622, p=0.017) and between HAX-1-positive fibroblasts and macrophages (Spearman's rho = 0.627, p=0.017). No correlations were found for mesothelium. An overview of correlations between gene proteins in adhesion tissue samples is shown in Table 7.

Discussion

Intra-abdominal adhesions, especially in infants, continue to be a big burden for both the patient and the medical staff. The information about this pathology, its morphological development and molecular mechanisms is quite limited, however, at the same time, the adhesion formation shares aspects with other fibrotic processes including activation of important signaling cascades and cellular transitions to myofibroblasts. This study discovered statistically significant differences between the number of immunopositive structures in control and adhesion group for SHH, IHH, FOXF1 and GATA4 and partially for GZMB.

Hedgehog signaling is thought to have an important role in regulating embryogenesis and tissue homeostasis. In this research a lack of both SHH and IHH expression was observed in the adhesion specimens while in literature the information is rather contradictory. Some reports state that loss of *IHH* initiates several events that are characteristic of an intestinal wound repair response, but prolonged loss resulted in progressive inflammation and the development of intestinal fibrosis with influx of fibroblasts and macrophages, and deposition of extracellular matrix proteins,[33]

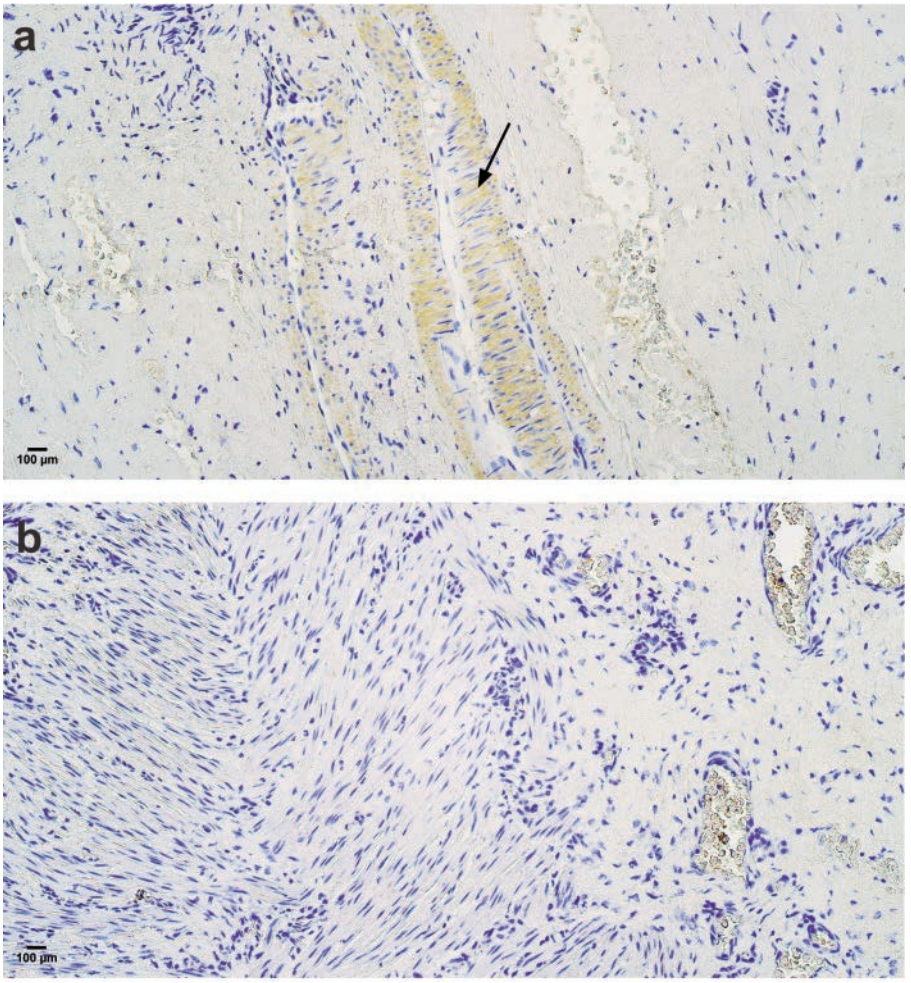

Figure 6. Immunopositive structures of HAX-1. **a**) Control sample with rare HAX-1 immunoreactive blood vessels (arrow), IHC HAX-1, x200. **b**) Adhesion sample with a lack of HAX-1 immunoreactivity, IHC HAX-1, x200.

while other researchers have reported quite the opposite - an upregulated *SHH* expression in other fibrosis affected organs, such as kidney, lungs and liver.[34-36] Hedgehog signaling pathway can be partially connected to other essential signaling cascades that are associated with fibrogenic effects, such as Wnt/b-catenin signaling and Notch signaling.[37] Through these pathways Snail1, a direct target and downstream mediator and a key transcription factor for mediating epithelial-mesenchymal transition and fibroblast migration, may be induced.[37,38] Alpha-smooth muscle actin (α-SMA) is another protein, partially controlled by Hedgehog signaling, that is associated with myofibroblast activation and matrix production.[37,39] It could be argued that while *SHH* and *IHH* expression is diminished, the fibrogenesis in the adhesion specimens could have occurred through other signaling pathways. It is known that loss of *IHH* signaling results in, for example, increased Wnt signaling.[33] However, the role of Hedgehog protein absence might be also associated with impaired cellular events like migration or apoptosis that result in altered peritoneal healing. Although the mesothelium did not exhibit widespread changes across all analyzed factors, the observed differences in SHH and IHH expression suggest that mesothelial Hedgehog signaling may contribute to adhesion-related remodeling, albeit to a much lesser extent than other structures. Notably, both SHH and IHH as components of the Hedgehog signaling pathway demonstrated strong correlations between fibroblasts and macrophages, indicating potential stromal-immune crosstalk during adhesion development. *FOXF1* has been described to be involved in midgut rotation and epithelial organization in the intestine. It is also identified as an anti-fibrotic factor that regulates key myofibroblast functions.[40] Our study revealed a significantly decreased expression of FOXF1 in the adhesion affected tissue, which is consistent with some other reports regarding the fibrogenesis in other organs. A lack of *FOXF1* in mice liver results in stimulated expression of pro-fibrotic genes.[41] Absence of *FOXF1* in mice endotheliocytes increases collagen deposition, myofibroblast activation and cytokine (IL-6, TNFα) secretion, which stimulates migration of macrophages. *FOXF1* deficiency is associated with impaired Ras-related protein (R-Ras) signaling, which is a direct transcriptional target of *FOXF1*.[42] R-Ras is important for blood vessel stabilization and maturation (it stimulates the signaling between endotheliocytes and pericytes), as well as regu-

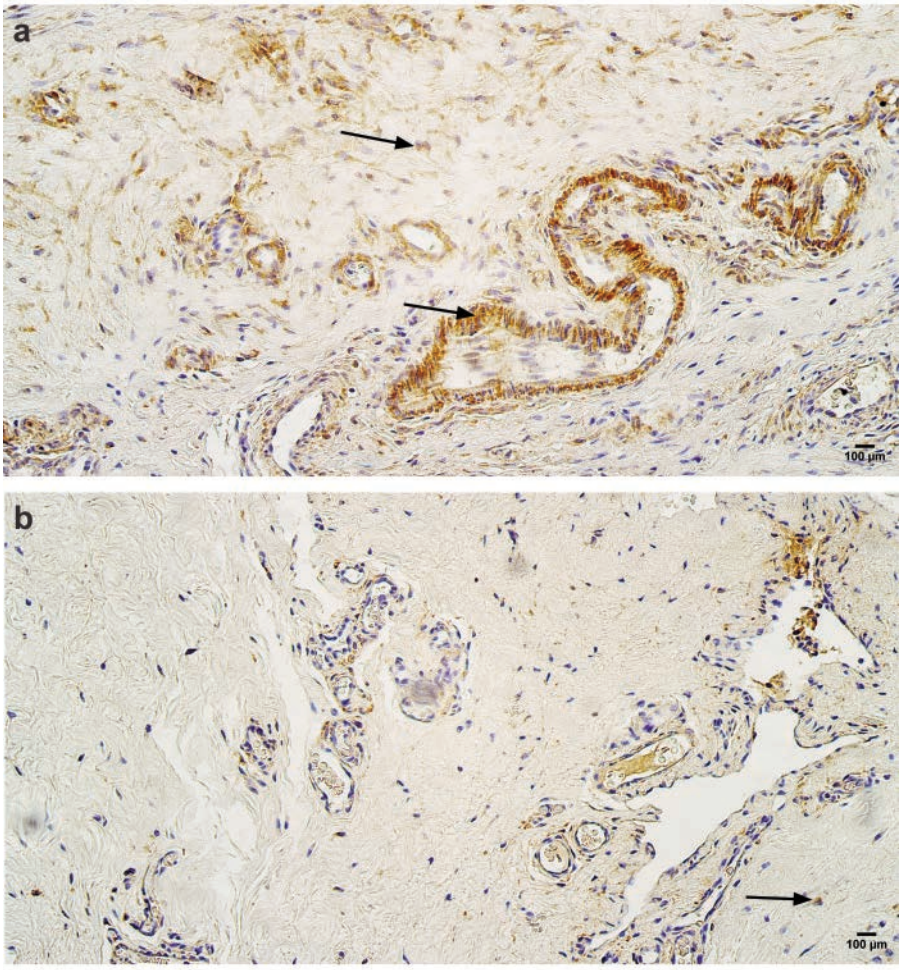

Figure 7. Immunopositive structures of GATA-4. **a**) Control sample with moderate number of GATA-4 immunopositive fibroblasts, macrophages and myocytes in blood vessels (arrows), IHC GATA-4, x200. **b**) Adhesion sample with a rare number of GATA-4 immunoreactive structures (arrow), IHC GATA-4, x200.

lation of different cellular events, for example, cell adhesion to the extracellular matrix through activation of integrin.[42,43] A lack of *FOXF1* and, therefore, a lack of R-Ras increases vascular permeability that can be involved in intensified fibrogenesis. *FOXF1* has been proven to be a part also in the hedgehog signaling pathway,[44] and in this study a statistically significant moderate positive correlation was observed between FOXF1 and SHH and IHH.

In the intestines it is thought that *GATA4* is responsible for jejunal-type enterocyte development and provides their functioning regarding intestinal absorption, however its role regarding fibrosis is still unclear. This study showed a significant downregulated expression of GATA4 in the adhesion group. Information about GATA4 functions and involvement in intestinal fibrogenic processes is very limited, but as for other organs yet again it is rather contradictory. For example, some reports say that in cardiac tissue changes of GATA4 expression has not shown any involvement in extra-cellular matrix accumulation,[45] while others have reported that inactivation of *GATA4* through the inhibition of extracellular signal-regulated kinases 1 and 2 (ERK1/2) signaling pathway attenuates cardiac hypertrophy and fibrosis.[46] Aberrant activation of ERK1/2 cascade is associated with peritoneal adhesion formation.[47] Interestingly, cell senescence has been reported to have beneficial effects for tissue and organs.[48] GATA4 signals to maintain cell senescence in heart, which together with CCN1 signaling pathway exerts anti-fibrosis effect.[49] It is worth mentioning that GATA4 is only one of the members of the GATA family of zinc-finger transcription factors, and many studies have shown that they can be partially or completely compensated by each other in several tissues and disease states.[26,50,51] Previously, an interaction of *GATA4* and *CDX2* (a paralog of *CDX1*) has been discovered, indicating their combinatory role in morphogenesis of intestinal development.[52] This study also observed a statistically significant high positive correlation between GATA-4 and CDX1.

GZMB is one of the most highly expressed granzymes both intra- and extracellularly and is currently known for its pro-apoptotic and pro-fibrotic effects.[53] It is responsible for proteolysis of fibronectin, decorin and VE-cadherin, which further contributes to the development of fibrosis. In cardiac fibrosis *GZMB* was found to be elevated,[54] however, our results showed a significant decrease in the number of GZMB-positive macrophages and blood vessels

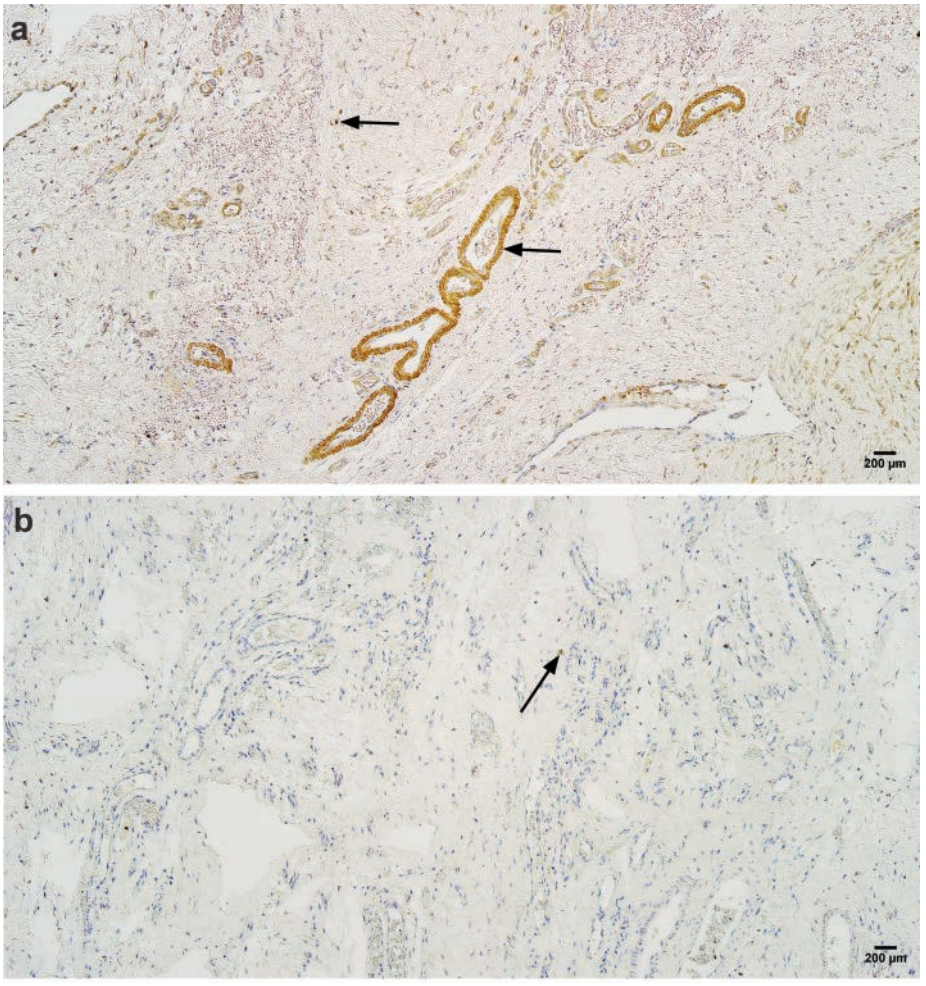

Figure 8. Immunopositive structures of GZMB. **a**) Control sample with moderate number of GZMB-immunopositive fibroblasts, macrophages and intensively stained myocytes in blood vessels (arrows), IHC GZMB, x100. **b)** Adhesion sample with rare occurring GZMB-immunoreactive structures (arrow), IHC GZMB, x100.

of intestinal adhesions. Data in literature about *GZMB* role in intestinal adhesion formation is scarce. Since this protein is considered a cytolytic factor, it could be argued that its expression is being downregulated physiologically in order to prevent too much damage in the already affected tissue, however the knowledge about exact mechanisms behind *GZMB* regulation is rather limited. Some studies have described the serine protease inhibitor b9 (serpinb9) as one of the GZMB secretion endogenous modulators, but due to its high sensitivity to oxidation it is most likely functioning only intracellularly, therefore suggesting that, when secreted, GZMB mostly remains in the tissue unregulated.[55] Experts say that GZMB located extracellularly is believed to have a significant influence on wound healing and fibrogenesis. Nonetheless, its interaction with its substrates and its involvement in different pathologies seem to vary greatly depending on the environment and circumstances, for example on the origin of the affected cells and the protein susceptibility to GZMB-driven cleavage.[53] Our findings of lack of GZMB in intestinal adhesions could also be possibly explained by granzyme polymorphism. However, more knowledge needs to be obtained in this matter and in GZMB molecular biology in general, since the information in the literature is very contradicting.[56]

CDX1 is an intestine-specific transcription factor involved in normal development and homeostasis of the gut. This study revealed no significant changes regarding CDX1 expression in adhesions, indicating that it does not play a key role in pathogenesis. A reduced *CDX1* expression can usually occur upon *CDX1* promoter hypermethylation which is present in malignant tumors, for example, colorectal carcinoma.[57]

HAX-1 in humans has at least 8 isoforms, and studies suggest there is a variability of its sub-localizations within the cells and functions.[58] In general, HAX-1 is described as a pleiotropic protein with main functions in regulating apoptosis.[59] In this study no significant changes were observed for HAX-1, except a slight decrease in blood vessels of intestinal adhesions, suggesting that it might not be involved in adhesion formation process. However, other reports have stated that in animal models inhibition of HAX-1 functions induces anti-inflammatory effects and results in decrease of fibrosis.[60]

Correlation analysis revealed a consistent pattern of strong positive associations among multiple factors across both stromal and vascular structures in adhesion tissue, which could suggest coordinated biological responses rather than isolated cell-specific changes, consistent with the complex multicellular nature of adhesion formation. Correlations between factors of immune/inflammatory related processes, like GZMB and HAX1, and developmental factors, such as GATA4 and CDX1, further suggest an interaction between inflammatory activity and developmental signaling pathways. This interplay may reflect an aberrant or persistent repair response contributing to adhesion formation and maintenance in the developing intestinal microenvironment.

Taking everything into account, the morphopathogenesis of infant adhesions is a multiplex process and based on this study it is characterized by a decreased expression of SHH, IHH, FOXF1, GATA4 and GZMB, which might be involved in aberrant developmental signaling cascades, inflammatory responses, possible vascular remodeling and other cellular events that lead to intensified fibrogenesis and intestinal adhesion formation. In order to gain a deeper insight into the mechanisms of this pathology and other involved factors, more research ought to be done.

Our manuscript possesses some limitations. There are relatively small adhesion and control groups. Additionally, only proteins were detected, which means that separate research should be made on gene level, and could be used to compare the findings. Also, it might be beneficial to separate and study specific type of adhesions - post-inflammatory and congenital ones, and to correlate this to the research data; and, finally, tissue factor concentration by usage of, for instance, ELISA method, could provide a more precise amount/level of the specific factor present during adhesion formation.

The diminished expression of FOXF1, GATA4, IHH and SHH suggests a dysregulation of the cellular proliferation, differentiation, migration and apoptosis of the main connective tissue cells fibroblasts and macrophages, also endothelium and blood vessel cells of infant adhesions. As for mesothelium, the present findings suggest it may play a limited and selective role in infant adhesion morphopathogenesis, particularly through Hedgehog-related signaling, rather than serving as a primary driver of adhesion formation.

GZMB, CDX1, HAX-1 appearance is similar in adhesions and control tissue, giving evidence about not significant role of these factors in infant adhesion development. Although, the slight tendency for GZMB to decrease in adhesions might indicate an impaired programmed cell death and inflammation/fibrosis stimulation in connective tissue.

Acknowledgements

The kind support of Rīga Stradiņš University is highly acknowledged. The authors would like to thank Assoc. Prof. Zane Ābola and Dr. med. Olafs Volrāts for providing the tissue samples.

References

1. Menzies D, Ellis H. Intestinal obstruction from adhesions - how big is the problem? Ann R Coll Surg Engl 1990;72:60-3.
2. Liao J, Li X, Fan Y. Prevention strategies of postoperative adhesion in soft tissues by applying biomaterials: based on the mechanisms of occurrence and development of adhesions. Bioact Mater 2023;26:387-412.
3. Erginel B, Soysal FG, Ozbey H, Keskin E, Celik A, Karadag A, et al. Small bowel obstruction due to anomalous congenital bands in children. Gastroenterol Res Pract 2016;2016: 7364329.
4. Zahn KB, Franz AM, Schaible T, Rafat N, Büttner S, Boettcher M, et al. Small bowel obstruction after neonatal repair of congenital diaphragmatic hernia - incidence and risk factors identified in a large longitudinal cohort study. Front Pediatr 2022;10:846630.
5. Lakshminarayanan B, Hughes-Thomas AO, Grant HW. Epidemiology of adhesions in infants and children following open surgery. Semin Pediatr Surg 2014;23:344-8.
6. Brüggmann D, Tchartchian G, Wallwiener M, Münstedt K, Tinneberg HR, Hackethal A. Intra-abdominal adhesions: definition, origin, significance in surgical practice, and treatment options. Dtsch Arztebl Int 2010;107:769-75.
7. Cheong YC, Laird SM, Li TC, Shelton JB, Ledger WL, Cooke ID. Peritoneal healing and adhesion formation/reformation. Hum Reprod Update 2001;7:556-66.
8. Choy SW, Cheng SH. Hedgehog signaling. Vitam Horm 2012;88:1-23.
9. Oldak M, Grzela T, Lazarczyk M, Malejczyk J, Skopinski P. Clinical aspects of disrupted hedgehog signaling. Int J Mol Med 2001;8:445-52.
10. Johnson RL, Tabin C. The long and short of hedgehog signa-

ling. Cell 1995;81:313-6.
11. van den Brink GR. Hedgehog signaling in development and homeostasis of the gastrointestinal tract. Physiol Rev 2007;87:1343-75.
12. Murone M, Rosenthal A, de Sauvage FJ. Sonic hedgehog signaling by the patched-smoothened receptor complex. Curr Biol 1999;9:76-84.
13. Katoh Y, Katoh M. Hedgehog target genes: mechanisms of carcinogenesis induced by aberrant hedgehog signaling activation. Curr Mol Med 2009;9:873-86.
14. Marigo V, Roberts DJ, Lee SM, Tsukurov O, Levi T, Gastier JM, et al. Cloning, expression, and chromosomal location of SHH and IHH: two human homologues of the Drosophila segment polarity gene hedgehog. Genomics 1995;28:44-51.
15. Madison BB, McKenna LB, Dolson D, Epstein DJ, Kaestner KH. FoxF1 and FoxL1 link hedgehog signaling and the control of epithelial proliferation in the developing stomach and intestine. J Biol Chem 2009;284:5936-44.
16. Malin D, Kim IM, Boetticher E, Kalin TV, Ramakrishna S, Meliton L, et al. Forkhead box F1 is essential for migration of mesenchymal cells and directly induces integrin-β3 expression. Mol Cell Biol 2007;27:2486-98.
17. Martin V, Shaw-Smith C. Review of genetic factors in intestinal malrotation. Pediatr Surg Int 2010;26:769-81.
18. Guo RJ, Suh ER, Lynch JP. The role of Cdx proteins in intestinal development and cancer. Cancer Biol Ther 2004;3:593-601.
19. Beck F, Stringer EJ. The role of Cdx genes in the gut and in axial development. Biochem Soc Trans 2010;38:353-7.
20. Neijts R, Amin S, van Rooijen C, Deschamps J. Cdx is crucial for the timing mechanism driving colinear Hox activation and defines a trunk segment in the Hox cluster topology. Dev Biol 2017;422:146-54.
21. Suzuki Y, Demoliere C, Kitamura D, Takeshita H, Deuschle U, Watanabe T. HAX-1, a novel intracellular protein localized on mitochondria, directly associates with HS1, a substrate of Src family tyrosine kinases. J Immunol 1997;158:2736-44.
22. Hippe A, Bylaite M, Chen M, von Mikecz A, Wolf R, Ruzicka T, et al. Expression and tissue distribution of mouse Hax1. Gene 2006;379:116-26.
23. Rubin DC. Intestinal morphogenesis. Curr Opin Gastroenterol 2007;23:111-4.
24. DeLaForest A, Kohlnhofer BM, Franklin OD, Stavniichuk R, Thompson CA, Pulakanti K, et al. GATA4 controls epithelial morphogenesis in the developing stomach to promote establishment of glandular columnar epithelium. Cell Mol Gastroenterol Hepatol 2021;12:1391-413.
25. Thompson CA, Wojta K, Pulakanti K, Rao S, Dawson P, Battle MA. GATA4 is sufficient to establish jejunal versus ileal identity in the small intestine. Cell Mol Gastroenterol Hepatol 2017;3:422-46.
26. Walker EM, Thompson CA, Battle MA. GATA4 and GATA6 regulate intestinal epithelial cytodifferentiation during development. Dev Biol 2014;392:283-94.
27. Jung K, Pawluk MA, Lane M, Nabai L, Granville DJ. Granzyme B in epithelial barrier dysfunction and related skin diseases. Am J Physiol Cell Physiol 2022;323:C170-9.
28. Frisch SM, Francis H. Disruption of epithelial cell-matrix interactions induces apoptosis. J Cell Biol 1994;124:619-26.
29. Velotti F, Barchetta I, Cimini FA, Cavallo MG. Granzyme B in inflammatory diseases: apoptosis, inflammation, extracellular matrix remodeling, epithelial-to-mesenchymal transition and fibrosis. Front Immunol 2020;11:587581.
30. Suvarna SK, Layton C, Bancroft JD. Bancroft's theory and practice of histological techniques. Amsterdam, Elsevier; 2019.
31. Junga A, Pilmane M, Ābola Z, Volrāts O. The morphopathogenetic aspects of intraabdominal adhesions in children under one year of age. Medicina (Kaunas) 2019;55:556.
32. Mukaka MM. Statistics corner: a guide to appropriate use of correlation coefficient in medical research. Malawi Med J 2012;24:69-71.
33. van Dop WA, Heijmans J, Büller NV, Snoek SA, Rosekrans SL, Wassenberg EA, et al. Loss of Indian hedgehog activates multiple aspects of a wound healing response in the mouse intestine. Gastroenterology 2010;139:1665-76.
34. Ding H, Zhou D, Hao S, Zhou L, He W, Nie J, et al. Sonic hedgehog signaling mediates epithelial-mesenchymal communication and promotes renal fibrosis. J Am Soc Nephrol. 2012;23:801-13.
35. Stewart GA, Hoyne GF, Ahmad SA, Jarman E, Wallace WA, Harrison DJ, et al. Expression of the developmental Sonic hedgehog (Shh) signalling pathway is upregulated in chronic lung fibrosis and the Shh receptor patched 1 is present in circulating T lymphocytes. J Pathol 2003;199:488-95.
36. Choi SS, Omenetti A, Syn WK, Diehl AM. The role of hedgehog signaling in fibrogenic liver repair. Int J Biochem Cell Biol 2011;43:238-44.
37. He W, Dai C. Key fibrogenic signaling. Curr Pathobiol Rep 2015;3:183-92.
38. He W, Kang YS, Dai C, Liu Y. Blockade of Wnt/β-catenin signaling by paricalcitol ameliorates proteinuria and kidney injury. J Am Soc Nephrol 2011;22:90-103.
39. Wang J, Zohar R, McCulloch CA. Multiple roles of alpha-smooth muscle actin in mechanotransduction. Exp Cell Res 2006;312:205-14.
40. Black M, Milewski D, Le T, Ren X, Xu Y, Kalinichenko VV, et al. FOXF1 inhibits pulmonary fibrosis by preventing CDH2-CDH11 cadherin switch in myofibroblasts. Cell Rep 2018;23:442-58.
41. Flood HM, Bolte C, Dasgupta N, Sharma A, Zhang Y, Gandhi CR, et al. The Forkhead box F1 transcription factor inhibits collagen deposition and accumulation of myofibroblasts during liver fibrosis. Biol Open 2019;8:bio039800.
42. Bian F, Lan YW, Zhao S, Deng Z, Shukla S, Acharya A, et al. Lung endothelial cells regulate pulmonary fibrosis through FOXF1/R-Ras signaling. Nat Commun 2023;14:2560.
43. Sawada J, Urakami T, Li F, Urakami A, Zhu W, Fukuda M, et al. Small GTPase R-Ras regulates integrity and functionality of tumor blood vessels. Cancer Cell 2012;22:235-49.
44. Madison BB, McKenna LB, Dolson D, Epstein DJ, Kaestner KH. FoxF1 and FoxL1 link hedgehog signaling and the control of epithelial proliferation in the developing stomach and intestine. J Biol Chem 2009;284:5936-44.
45. Dittrich GM, Froese N, Wang X, Kroeger H, Wang H, Szaroszyk M, et al. Fibroblast GATA-4 and GATA-6 promote myocardial adaptation to pressure overload by enhancing cardiac angiogenesis. Basic Res Cardiol 2021;116:26.
46. Shu C, Chen C, Zhang DP, Guo H, Zhou H, Zong J, et al. Gastrodin protects against cardiac hypertrophy and fibrosis. Mol Cell Biochem 2012;359:9-16.
47. Jin X, Ren S, Macarak E, Rosenbloom J. Pathobiological mechanisms of peritoneal adhesions: the mesenchymal transition of rat peritoneal mesothelial cells induced by TGF-β1 and IL-6 requires activation of Erk1/2 and Smad2 linker region phosphorylation. Matrix Biol 2016;51:55-64.
48. Muñoz-Espín D, Serrano M. Cellular senescence: from physiology to pathology. Nat Rev Mol Cell Biol 2014;15:482-96.

49. Cui S, Xue L, Yang F, Dai S, Han Z, Liu K, et al. Postinfarction hearts are protected by premature senescent cardiomyocytes via GATA4-dependent CCN1 secretion. J Am Heart Assoc 2018;7:e009111.
50. van Berlo JH, Elrod JW, van den Hoogenhof MM, York AJ, Aronow BJ, Duncan SA, et al. The transcription factor GATA-6 regulates pathological cardiac hypertrophy. Circ Res 2010;107:1032-40.
51. Haveri H, Westerholm-Ormio M, Lindfors K, Mäki M, Savilahti E, Andersson LC, et al. Transcription factors GATA-4 and GATA-6 in normal and neoplastic human gastrointestinal mucosa. BMC Gastroenterol 2008;8:9.
52. Boudreau F, Rings EH, van Wering HM, Kim RK, Swain GP, Krasinski SD, et al. Hepatocyte nuclear factor-1 alpha, GATA-4, and caudal related homeodomain protein Cdx2 interact functionally to modulate intestinal gene transcription: implication for the developmental regulation of the sucrase-isomaltase gene. J Biol Chem 2002;277:31909-17.
53. Turner CT, Hiroyasu S, Granville DJ. Granzyme B as a therapeutic target for wound healing. Expert Opin Ther Targets 2019;23:745-54.
54. Shen Y, Cheng F, Sharma M, Merkulova Y, Raithatha SA, Parkinson LG, et al. Granzyme B deficiency protects against angiotensin II-induced cardiac fibrosis. Am J Pathol 2016;186:87-100.
55. Kaiserman D, Bird PI. Control of granzymes by serpins. Cell Death Differ 2010;17:586-95.
56. Susanto O, Trapani JA, Brasacchio D. Controversies in granzyme biology. Tissue Antigens 2012;80:477-87.
57. Pilozzi E, Onelli MR, Ziparo V, Mercantini P, Ruco L. CDX1 expression is reduced in colorectal carcinoma and is associated with promoter hypermethylation. J Pathol 2004;204:289-95.
58. Lees DM, Hart IR, Marshall JF. Existence of multiple isoforms of HS1-associated protein X-1 in murine and human tissues. J Mol Biol 2008;379:645-55.
59. Yedavalli VS, Shih HM, Chiang YP, Lu CY, Chang LY, Chen MY, et al. Human immunodeficiency virus type 1 Vpr interacts with antiapoptotic mitochondrial protein HAX-1. J Virol 2005;79:13735-46.
60. Zhang T, Zhang Y, Li S, Ge H, Song Q, Zhang Y, et al. Gentianella acuta-derived Gen-miR-1 suppresses myocardial fibrosis by targeting HAX1/HMG20A/Smads axis to attenuate inflammation in cardiac fibroblasts. Phytomedicine 2023;118:154923.

Received: 31 October 2025. Accepted: 21 January 2026.

European Journal of Histochemistry 2026; 70:4438
doi:10.4081/ejh.2026.4438